Supporting Information

Lithium diisopropylamide-mediated aldol condensation of ethyl acetate and 3-pyridine aldehyde: batch limitations and advantages of continuous processing

Letao Guo[a,b], Mei Yang[a,*], Lixia Yang[a], Mei Han[a], Wenna Tang[a], Guangwen Chen[a,*]

a. Dalian Institute of Chemical Physics, Chinese Academy of Sciences, Dalian 116023, China

b. University of Chinese Academy of Sciences, Beijing 100049, China

[*] Corresponding author. Tel.: +86-411-8437-9031, Fax.: +86-411-8469-1570

E-mail address: yangmei@dicp.ac.cn; gwchen@dicp.ac.cn. ORCID Guangwen Chen: 0000-0001-5290-7921

1. Details of HPLC analysis

HPLC Column type: C18, Φ 4.6×150 mm, 5 μm particle size (Agilent PN 773450-902). All quantitative characterization was performed using the external standard method.

β-hydroxy ester 3b (tert-butyl 3-hydroxy-(3-pyridyl) propanoate)

Mobile phase: 30 vol% 0.1 wt% aqueous formic acid (Mobile phase 1) - 70 vol% methanol (Mobile phase 2); **Injection sample:** 5 μl; **Flow rate:** 1 ml·min^{-1}; **Wavelength of UV detector:** 250 nm; **Column temperature:** 20 °C; **Retention time:** 1.6-1.7 min.

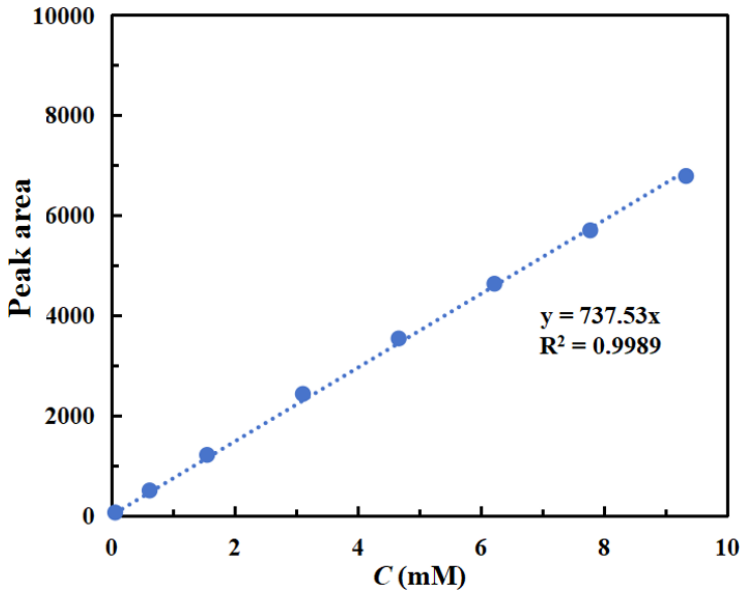

Figure S1. External standard curve of tert-butyl 3-hydroxy-(3-pyridyl)propanoate

Aldehyde 2a (3-pyridine aldehyde)

Mobile phase: 50 vol% methanol (Mobile phase 1) - 50 vol% acetonitrile (Mobile phase 2); **Injection sample:** 5 μl; **Flow rate:** 1 ml·min^{-1}; **Wavelength of UV detector:** 250 nm; **Column temperature:** 20 °C; **Retention time:** 1.4-1.5 min.

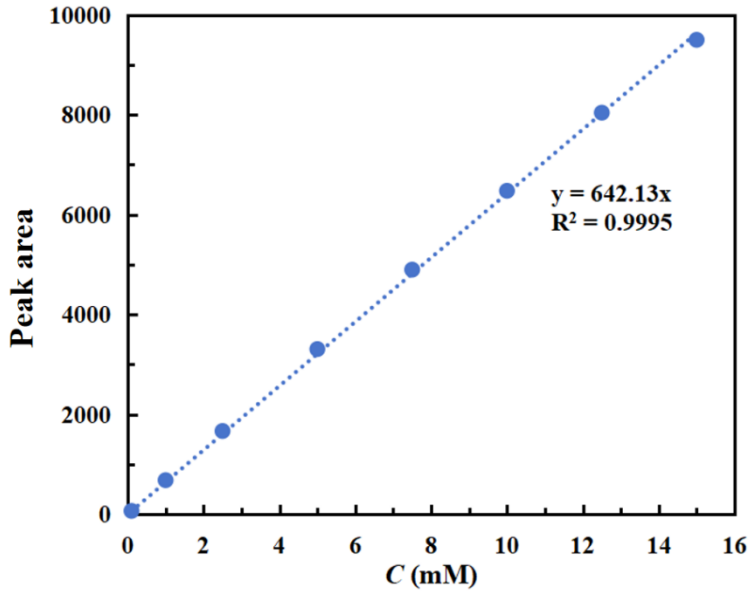

Figure S2. External standard curve of 3-pyridine aldehyde

β-hydroxy ester 3a (ethyl 3-hydroxy-3-(pyridin-3-yl)propanoate)

Mobile phase: 70 vol% 0.1 wt% aqueous formic acid (Mobile phase 1) - 30 vol% methanol (Mobile phase 2); **Injection sample:** 5 μL; **Flow rate:** 1 mL/min; **Wavelength of UV detector:** 250 nm; **Column temperature:** 20 °C; **Retention time:** 1.67-1.71 min.

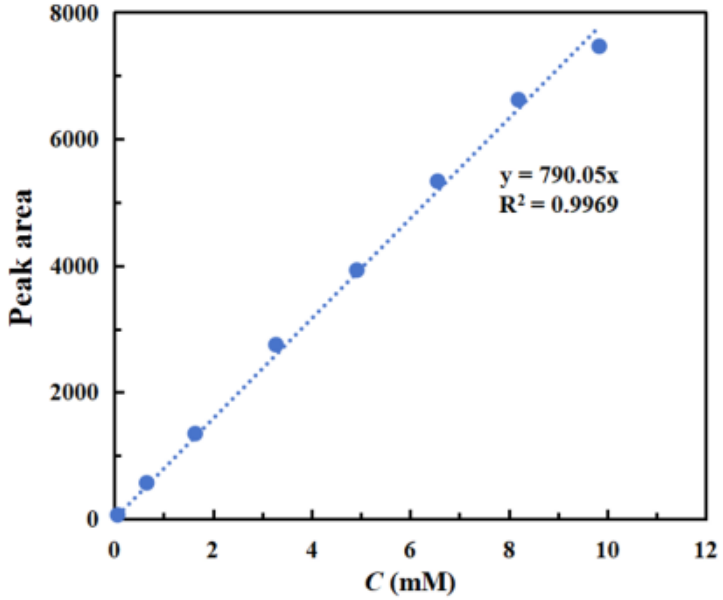

Figure S3. External standard curve of ethyl 3-hydroxy-3-(pyridin-3-yl)propanoate

2. The ^{1}H NMR quantification of ester-enolate behaviour

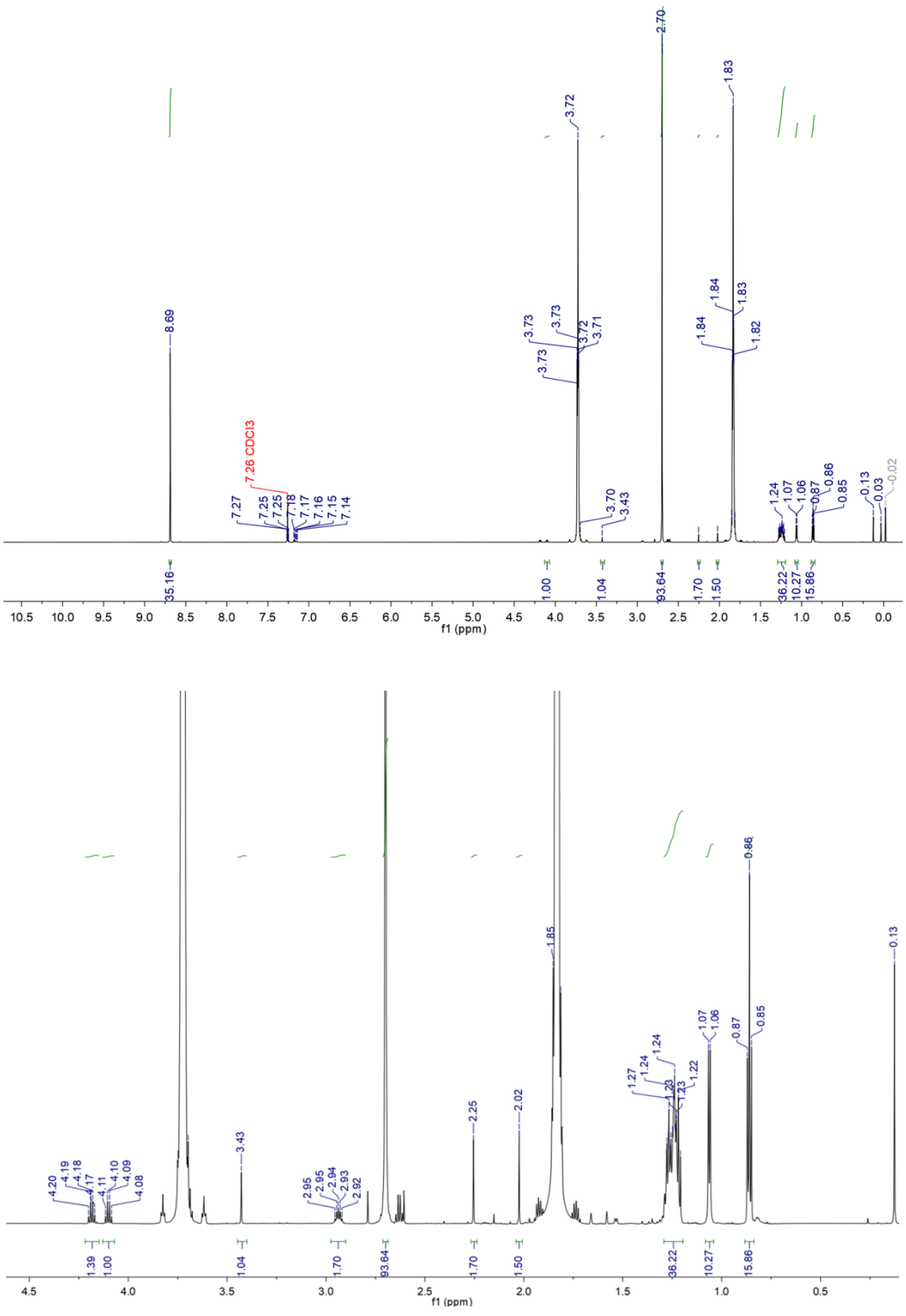

Figure S4. Quantitative ^{1}H NMR characterization of the organic phase without solvent removal (in $CDCl_3$)

Table S1. Summary of the ^{1}H NMR peak assignments in Fig. S4 ($CDCl_3$)

Compound	Chemical shift (ppm)	Chemical shift of pure reagents [a] (ppm)
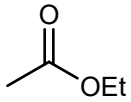	Overlapping with other peaks (OCH_2CH_3)	1.23 (OCH_2CH_3)
	2.02 (CH_3CO)	2.01 (CH_3CO)
	4.08 (OCH_2CH_3)	4.09 (OCH_2CH_3)
 **(solvent)**	1.83	-
	3.72	-
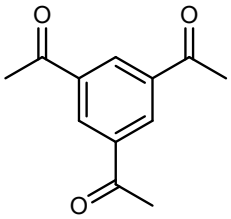 **(internal standard substance)**	2.70 (CH_3CO)	2.71 (CH_3CO)
	8.69 (ph-H)	8.71 (ph-H)
 **(solvent from commercial LDA solution)**	0.86 (CH_2CH_3)	0.88 (CH_2CH_3)
	Overlapping with other peaks 1.23-1.3 (CH_2CH_3)	1.2-1.33 (CH_2CH_3)
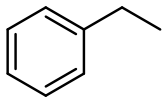 **(solvent from commercial LDA solution)**	Overlapping with other peaks (CH_2CH_3)	1.24 (CH_2CH_3)
	Overlapping with other peaks (CH_2CH_3)	2.65 (CH_2CH_3)
	7.14-7.27 (ph-H)	7.12-7.28 (ph-H)
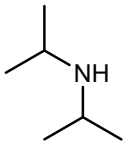	1.07 ($CHCH_3$)	1.0 ($CHCH_3$)
	2.94 ($CHCH_3$)	2.93-2.79 ($CHCH_3$)
	Overlapping with other peaks (OCH_2CH_3)	1.16 (OCH_2CH_3)
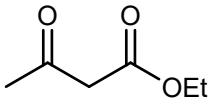	2.25 ($COCH_3$)	2.14 ($COCH_3$)
	3.43 ($COCH_2CO$)	3.34 ($COCH_2CO$)
	4.19 (OCH_2CH_3)	4.07 (OCH_2CH_3)
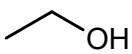	Overlapping with other peaks (OCH_2CH_3)	1.24 (OCH_2CH_3)
	Overlapping with other peaks (OCH_2CH_3)	3.7 (OCH_2CH_3)

3. The details of mass spectrum

3.1 The overview of the byproducts via MS characterization

Mass spectrometer parameter settings: ESI positive mode, frag-mentor voltage: 180 V

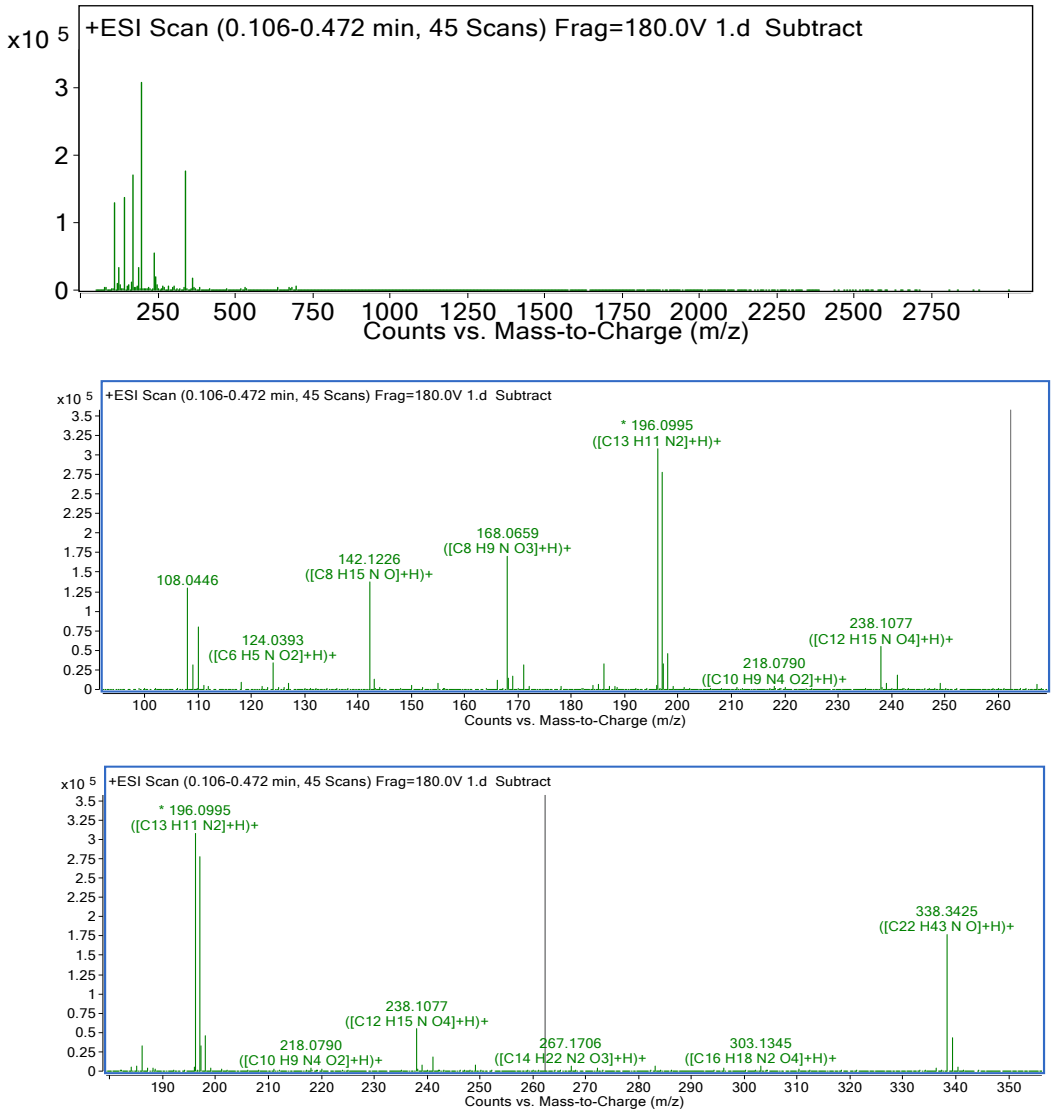

Figure S5. The mass spectrum of the organic phase obtained via batch operation at -60 ºC. The proposed molecular structures were assigned using the instrument's built-in analysis software.

Table S2. Summary of peaks with m/z less than 300 (major ion peaks are labeled in red, while peaks with intensities exceeding 10000 are highlighted in bold to enhance visual clarity)

m/z	Intensity	m/z	Intensity	m/z	Intensity
80.0495	3403.03	**166.0863**	**12099.44**	**196.2232**	**37580.9**
81.9376	3144.69	**168.0659**	**170241.94** (5)	**196.2421**	**22103.85**
108.0446	**129485.6** (1)	168.0799	2603.43	**196.2559**	**13524.14**
108.0555	2859.06	**168.0914**	**14001.76**	196.2759	8581.74
108.0652	9675.71	**169.0689**	**17323.47**	197.0812	3814.37
109.0517	**31742.01**	**171.0917**	**30943.77**	**197.1016**	**278044.34**
110.0601	**79828.87** (2)	171.1052	3110.66	**197.1282**	**32774.46**
110.0712	3984.32	171.1176	2041.26	**197.1426**	**13320.74**
110.081	4612.38	172.0951	3946.76	**197.1619**	**15092.03**
111.0634	5793.77	178.0864	3782.64	**197.1834**	**14916.68**
112.0216	4397.35	184.1333	4963.27	**198.1025**	**45402.79**
118.1226	9759.79	185.1081	6151.56	198.1292	2242.9
122.0599	4316.59	**186.1152**	**32901.16**	199.1053	3273.53
122.964	3132.23	186.1291	3331.64	201.1064	2552.54
124.0393	**33407.73** (3)	186.1432	2234.18	211.0942	2294.67
124.0511	2796.56	187.1186	4380.13	218.079	3683.89
125.0427	2435.11	188.1645	3487.1	220.097	3207.85
126.0913	2710.81	188.6484	2249.08	**238.1077**	**55005.15** (7)
127.0389	8445.57	196.0808	5145.9	238.1236	2360.52
142.1226	**137056.06** (4)	**196.0995**	**307996.81** (6)	239.1109	7352.44
142.1353	3830.77	**196.1135**	**217253.95**	**241.1049**	**18874.88**
142.1462	7584.09	**196.1245**	**30296.3**	241.1203	2017.86
143.126	**13337.68**	**196.1393**	**27536.22**	249.1599	7610.73
144.0807	1999.27	**196.1574**	**179445.63**	267.1706	6486.89
150.0546	5604.72	**196.179**	**140125.77**	272.1858	3942.66
155.0703	7467.19	**196.2085**	**33485.39**	296.1496	3533.83

Table S3. Summary of proposed molecular structures

Compounds	m/z Calculated $[M+H]^+$	m/z Found	Error (ppm)	Corresponding peak [a]
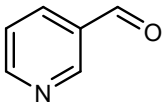	$[C_6H_5NO+H]^+$ 108.0444	108.0446	+1.8	**1**
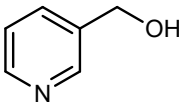	$[C_6H_7NO+H]^+$ 110.06	110.0601	+0.9	**2**
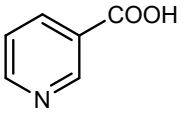	$[C_6H_5NO_2+H]^+$ 124.0393	124.0393	0	**3**
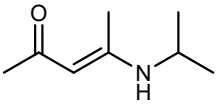	$[C_8H_{15}NO+H]^+$ 142.1226	142.1226	0	**4**
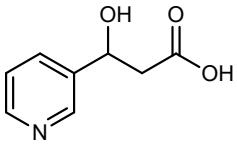	$[C_8H_9NO_3+H]^+$ 168.0655	168.0659	+2.4	**5**
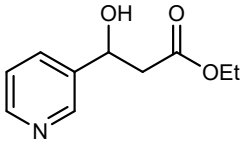	$[C_{10}H_{13}NO_3+H]^+$ 196.0968	196.0995	+13.8	**6**
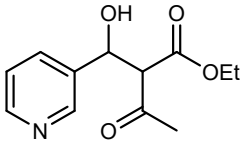	$[C_{12}H_{15}NO_4+H]^+$ 238.1074	238.1077	+1.3	**7**

Note: [a] The corresponding ion peaks were labeled in Table S2.

3.2 The separation of byproducts B3 via GC-MS

Mass spectrometer parameter settings: ESI mode, frag-mentor voltage: 180 V. The proposed molecular structures were assigned using the instrument's built-in analysis software.

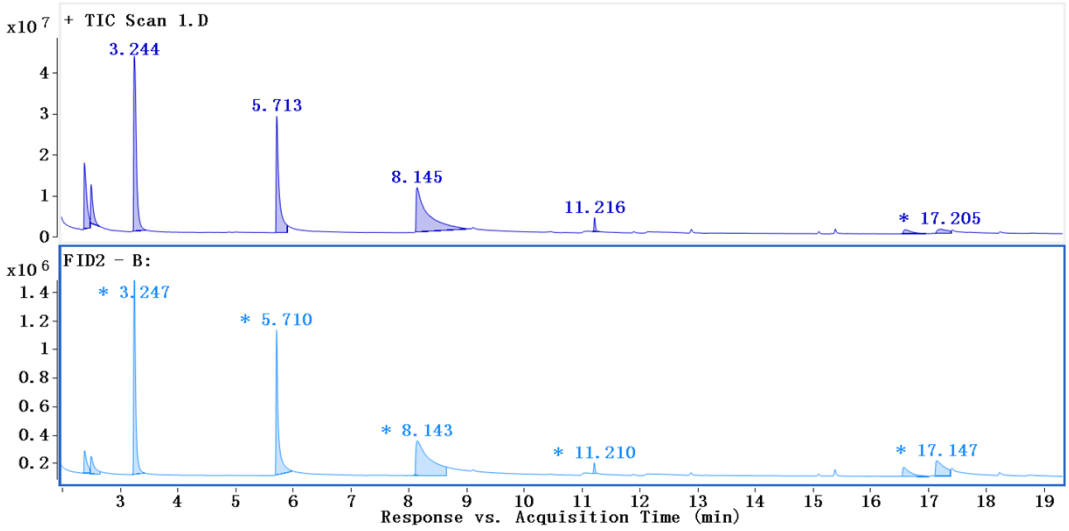

Peak	Start (min)	RT (min)	End (min)	Height	Area	Area %
1	2.37	2.383	2.482	16040014.12	50589978.76	10.27
2	2.482	2.499	2.643	9443251.94	26450983.12	5.37
3	3.228	3.244	3.459	42567833.17	134658478.7	27.34
4	5.691	5.713	5.899	28338388.76	100011169.5	20.31
5	8.112	8.145	9.063	10805909.23	152625635	30.99
6	11.183	11.216	11.316	3445720.92	6006552.31	1.22
7	16.536	16.593	16.952	979699.55	9185728.97	1.87
8	17.115	17.205	17.388	1044769.44	12915734.4	2.62

Figure S6. GC-MS characterization details

Identified compound 1: Ethyl acetate (extractant present in the reaction mixture for MS characterization) (Retention time: 2.373 min).

Identified compound 2: Tetrahydrofuran (solvent present in the reaction mixture for MS characterization) (Retention time: 2.489 min).

Identified compound 3: Tert-butyl acetate (Retention time: 3.234 min)

Identified compound 4: Toluene (solvent present in commercial LDA solution) (Retention time: 5.7 min)

Identified compound 5: 3-pyridine aldehyde **(2a)** (Retention time: 8.125 min)

Identified compound 6: the main byproduct observed in bath operation

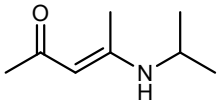

[$C_8H_{15}NO$] calculated [M] 141.1148

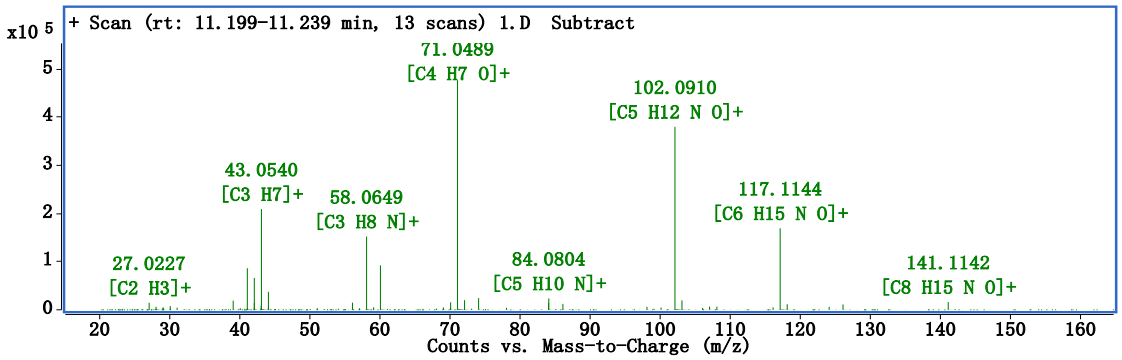

Figure S7. Mass spectrum obtained by GC-MS (Retention time: 11.2 min).

4. Villermaux-Dushman method

To get more details about the mixing performance on the microscale, the Villermaux-Dushman method was employed, including the following parallel competing reactions:

$$H_2BO_3^- + H^+ \rightarrow H_3BO_3 \ (quasi-instantaneous)$$

$$IO_3^- + 5I^- + 6H^+ \rightarrow 3I_2 + 3H_2O \ (very\ fast)$$

$$I_2 + I^- \rightarrow I_3^- \ (instantaneous\ equilibrium\ reaction)$$

The neutralisation of $H_2BO_3^-$ ions is quasi-instantaneous, while the Dushman reaction is much slower than the neutralisation reaction, but in the same characteristic time scale with the micromixing process. As for perfect mixing, the H^+ ions are instantaneously consumed by $H_2BO_3^-$ ions. The Dushman reaction cannot happen due to the stoichiometric defect of H^+ ions. In the case of imperfect mixing, a local stoichiometric excess of H^+ ions whose amount is larger than that required by neutralisation of $H_2BO_3^-$ ions exists. Therefore, the H^+ ions are consumed competitively by the neutralisation of $H_2BO_3^-$ ions and the Dushman reaction. The formed I_2 further reacts with I^- ions to yield I_3^- ions. The amount of produced I_3^- ions depends on the micromixing efficiency and can be monitored by a UV-Vis spectrophotometer (UV2700, Shimadzu, Japan) at 353 nm. The extinction coefficient of I_3^- was 25505 $L \cdot mol^{-1} \cdot cm^{-1}$ measured in this study.

All the experiments were carried out at room temperature (20 °C). In a typical experimental procedure, a solution containing H_3BO_3, NaOH, KI and KIO_3 (Solution A) and a diluted H_2SO_4 solution (Solution B) were prepared separately. The mixed solution and the H_2SO_4 solution were independently introduced into M1 using syringe pumps. The experimental procedure followed that illustrated in Fig. 3, except that the continuous-flow platform used for mixing performance evaluation consisted only of M1 and C1. After the system reached steady state, the reaction effluent was collected at the outlet and its absorbance at 353 nm was measured within 1 min using a UV-vis spectrophotometer (UV2700, Shimadzu, Japan). Based on the obtained concentration of I_3^- ions, the segregation index (X_s) which was defined to quantify the micromixing performance could be calculated by above equations:

$$X_s = \frac{Y}{Y_{ST}}$$

$$Y = \frac{2(V_A + V_B)([I_2] + [I_3^-])}{V_B[H^+]_0}$$

$$Y_{ST} = \frac{6[IO_3^-]_0}{6[IO_3^-]_0 + [H_2BO_3^-]_0} \quad \text{(S1-S3)}$$

where Y denotes the ratio of the mole number of acid consumed by the Dushman reaction to the total mole number of the H^+ ions injected. Y_{ST} is the value of Y in the total segregation when the micromixing process is infinitely slow. In this case, the H^+ ions are proportionally consumed by the $H_2BO_3^-$ ions and I^-/IO_3^- ions according to their local concentrations. V_A and V_B are the volumetric flow rates of the mixed solution and H_2SO_4 solution, respectively. $[I_2]$ and $[I_3^-]$ are the concentrations of I_2 and I_3^- ions in the reaction effluent, while $[H^+]_0$ is the initial concentration of H^+ ions in H_2SO_4 solution, and $[IO_3^-]_0$ and $[H_2BO_3^-]_0$ are the initial concentrations of IO_3^- and $H_2BO_3^-$ ions in the mixed solution. The value of X_s equals to 0 for perfect mixing state, while X_s is 1 for complete segregated state.

Table S4 The composition of mixing solution (Solution A) and H_2SO_4 solution (Solution B)

Compound	Concentration (M)
H_3BO_3 **(A)**	0.2
NaOH **(A)**	0.1
KI **(A)**	0.0116
KIO_3 **(A)**	0.00223
H_2SO_4 **(B)**	0.02

According to the study of Yang et al. *(Ind. Eng. Chem. Res.,* 2005, **44**, 7730-7737), for incorporation model, a limited fluid, acid, is divided into aggregates and progressively invaded by environmental fluid that contains iodide and iodate in a basic medium. Acid aggregates grow by progressively incorporating the surrounding medium where neutralisation of $H_2BO_3^-$ ions and Dushman reaction take place. The characteristic time of incorporation, t_m, is assumed to be equal to the micromixing time. The volume of the aggregate grows according to following equation:

$$V_2 = V_{20}g(t) \quad \text{S4}$$

where V_2 is the volume of the acid aggregate, V_{20} is the initial volume of the acid aggregate, and g(t) is the incorporation function with the form:

$$g(t) = exp(t/\tau_m) \text{ or } g(t) = 1 + t/\tau_m \quad \text{S5}$$

where τ_m is the characteristic micromixing time.

The concentrations of the j species can be calculated by the following equation:

$$\frac{dC_j}{dt} = (C_{j10} - C_j)\frac{1}{g}\frac{dg}{dt} + R_j \quad \text{S6}$$

where subscript 10 represents the surrounding fluid and R_j is the net production rate of species j (j=$H_2BO_3^-$, H^+, I^-, IO_3^-, I_2 or I_3^-) for the reaction. When $g(t) = \exp(t/\tau_m)$, Equation S6 can be transformed to:

$$\frac{dC_j}{dt} = \frac{C_{j10} - C_j}{\tau_m} + R_j \quad \text{S7}$$

With a series of presumed value of micromixing time and known initial concentration of different ions in each solution, Equation S7 could be solved by MATLAB (ode15s). The value of time step was fixed at 10^{-8} s, and the integration process was terminated when the H^+ ions were completely consumed with 10^{-8} M as the criterion.

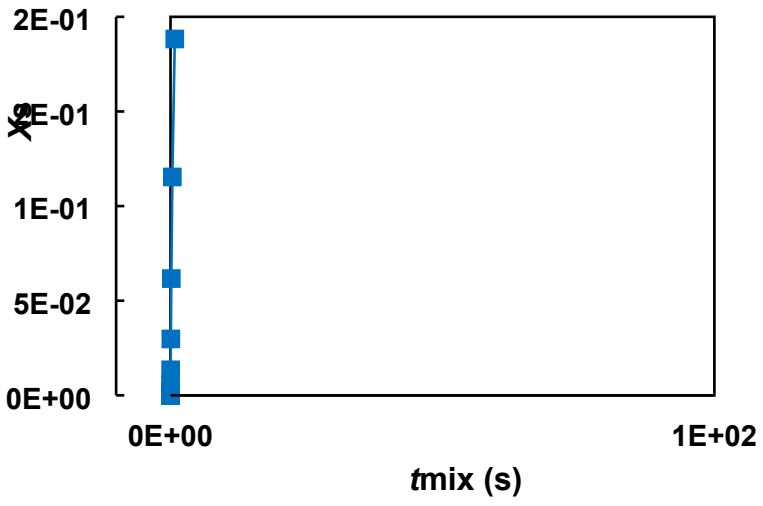

Figure S8. Relationship between micromixing time and segregation index obtained from

incorporation model.

5. Other additional experimental data

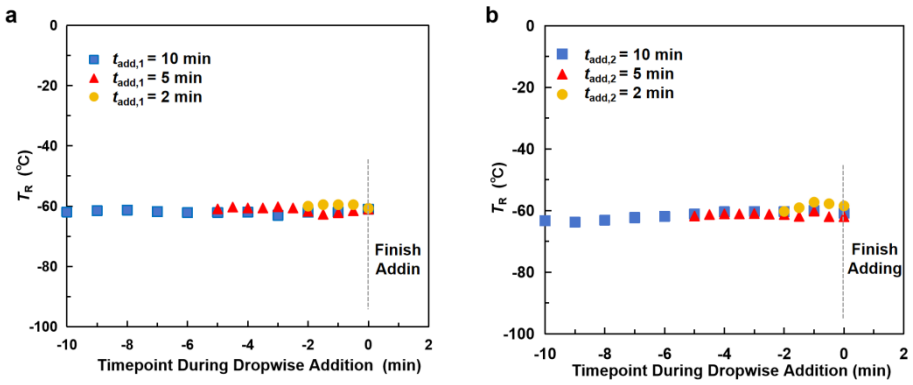

Figure S9. Temperature profiles recorded during rapid addition of the ester-THF and **2a**-THF solutions. (a) The recorded temperature during different addition time of the ester-THF corresponding to the Fig. 4a. (b) The recorded temperature during different addition time of the aldehyde-THF corresponding to the Fig. 5a.

The space time yield (STY)

For the batch operation, the STY was calculated according to the following equation:

$$\mathrm{STY} = \frac{m_\mathrm{p}}{t_\mathrm{R} \times V_\mathrm{R}} = \frac{C_\mathrm{EA} \times V_\mathrm{EA} \times \mathrm{MW}_\mathrm{3a} \times Y_\mathrm{3a}}{t_\mathrm{R} \times V_\mathrm{R}} \qquad \text{S8}$$

where m_p is the mass of product **3a**, t_R is the total operation time including dropwise addition and reaction (t_R = 45 min), V_R is the total reaction volume (V_R = 60 mL), C_EA is the concentration of EA in EA-THF solution (C_EA = 0.5 M), V_1 is the volume of EA-THF solution (V_EA = 20 mL), MW_3a is the molecular weight of **3a** (MW_3a = 195 g/mol), and Y_3a was the yield of **3a**.

For the continuous-flow operation, the STY was calculated according to the following equation:

$$\mathrm{STY} = \frac{C_\mathrm{EA} \times Q_\mathrm{EA} \times \mathrm{MW}_\mathrm{3a} \times Y_\mathrm{3a}}{V_\mathrm{C1} + V_\mathrm{C2}} \qquad \text{S9}$$

where V_{C1} and V_{C2} were the volumes of the capillary C1 and C2, respectively. Q_{EA} was the flow rate of EA-THF solution.

E-factor

The E-factor was calculated according to the following equation:

$$\text{E - factor} = \frac{\sum m_{\text{input}} - m_{\text{product}}}{m_{\text{product}}} \quad \text{S10}$$

where m corresponds to the mass (expressed in g).

Table S5 Batch operation (C_{LDA} = 1.0 M, C_{EA} = C_{2a} = 0.5 M)

Considering 60 mL total volume

Compound	Mass (g)
n-Heptane	2.63
Ethyl benzene	1.33
THF	49.09
Ethyl acetate	0.88
3-pyridine aldehyde	1.07
LDA	2.15
H_2O	60
NH_4Cl	22.32
Na_2SO_4	11.7
Total	151.17

Table S6 Continuous-flow operation (C_{LDA} = 0.6 M, C_{EA} = C_{2a} = 0.5 M, Q_{LDA} = Q_{EA} = Q_{2a} = 2 mL/min)

Considering a 10 min operation

Compound	Mass (g)
n-Heptane	1.58
Ethyl benzene	0.8
THF	49.09
Ethyl acetate	0.88
3-pyridine aldehyde	1.07
LDA	1.29
H_2O	60
NH_4Cl	22.32
Na_2SO_4	11.7
Total	148.73

Process mass intensity (PMI)

The PMI was calculated according to the following equation:

$$\mathrm{PMI} = \frac{\sum m_{\mathrm{input}}}{m_{\mathrm{product}}} = \mathrm{E-factor} + 1 \qquad \text{S11}$$

where m corresponds to the mass (expressed in g).

6. The separation of byproduct B2

Pyridin-3-ylmethanol (separated from aldol condensation byproducts)

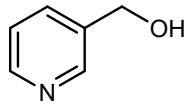

Separation details

The byproduct **B2** was also separated in our previous research (Guo et al. *Chen, Chin. J. Chem. Eng.*DOI: 10.1016/j.cjche.2025.10.011). Herein, we tried to separate it again and the byproduct **B2** can also be observed in reaction mixture via batch operation by TLC monitor. Through silica gel chromatographic separation, we obtained the **B2** with pale yellow oil. After removing solvent, the mixture was characterized by ^{1}H NMR.

Characterization data:

^{1}H NMR (400 MHz, d6-DMSO) δ 8.52 (d, *J* = 2.2 Hz, 1H), 8.45 (dd, *J* = 4.8, 1.7 Hz, 1H), 7.72 (dt, *J* = 7.8, 2.1 Hz, 1H), 7.34 (ddd, *J* = 7.8, 4.8, 0.9 Hz, 1H), 4.53 (s, 2H) ppm.

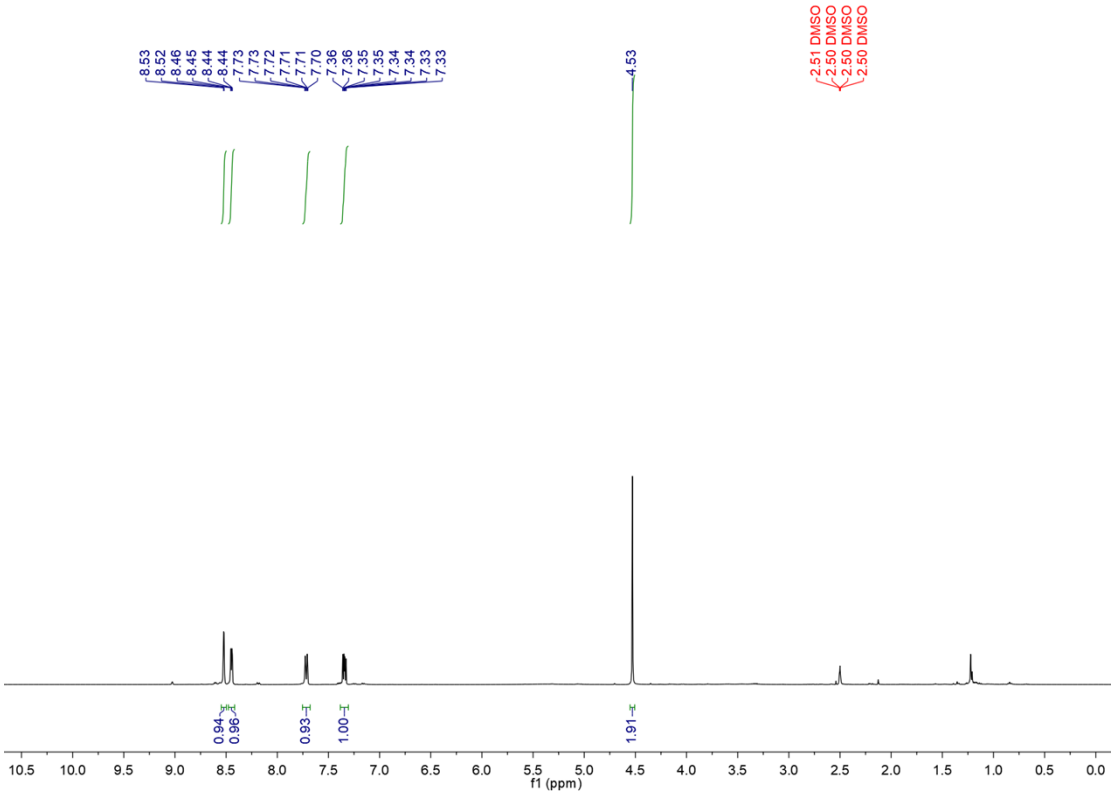

7. ^{1}H Characterization of aldol condensation products

Ethyl 3-hydroxy-3-phenylpropanoate (3c)

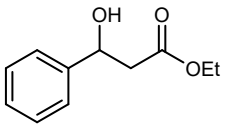

Characterization data:

^{1}H NMR (700 MHz, Chloroform-d) δ 7.40 - 7.22 (m, 5H), 5.11 (dd, *J* = 9.3, 3.7 Hz, 1H), 4.16 (q, *J* = 7.2 Hz, 2H), 2.76 - 2.64 (m, 2H), 1.24 (t, *J* = 7.2 Hz, 3H) ppm.

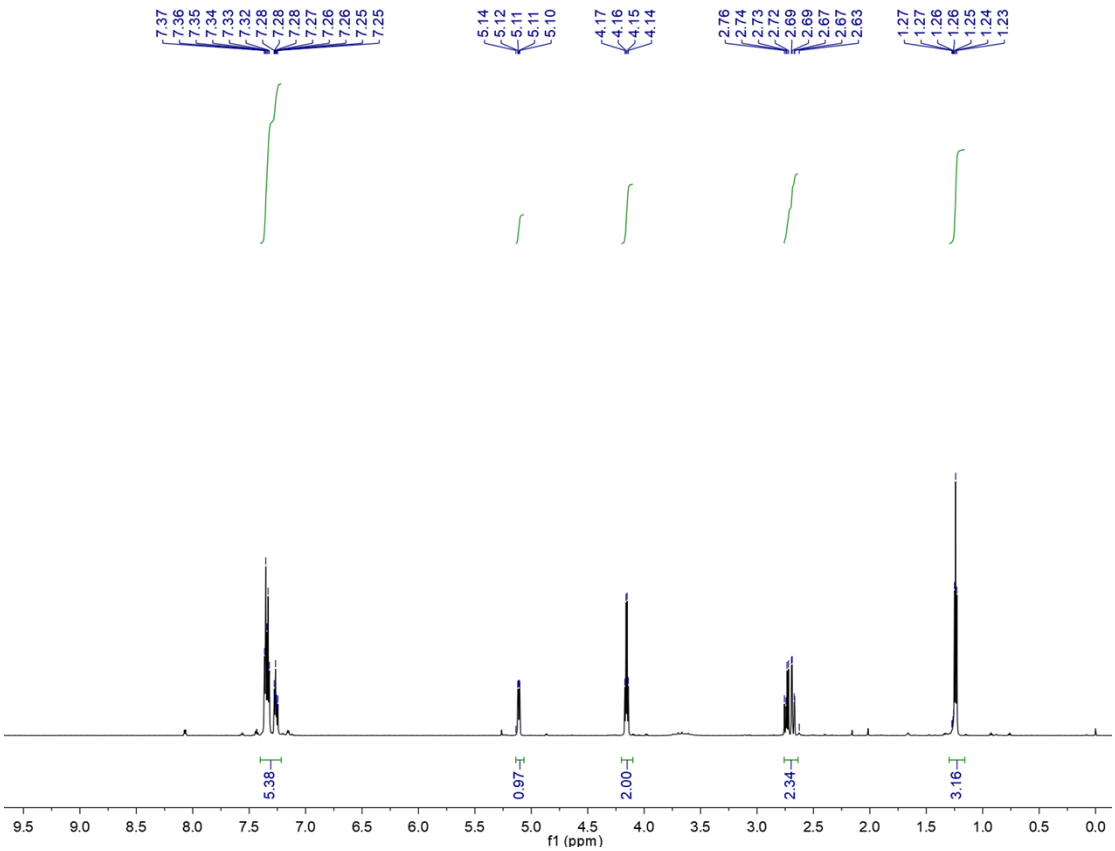

Ethyl 3-hydroxypent-4-enoate (3d)

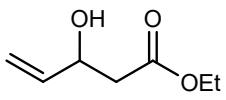

Characterization data:

^{1}H NMR (700 MHz, Chloroform-d) δ 5.86 (ddd, *J* = 16.7, 10.5, 5.5 Hz, 1H), 5.29 (dd, *J* = 17.2, 1.7 Hz, 1H), 5.12 (dd, *J* = 10.5, 1.7 Hz, 1H), 4.15 (q, *J* = 7.1 Hz, 2H), 2.58 - 2.44 (m, 2H), 1.24 (t, *J* = 7.2 Hz, 3H) ppm.

^{13}C NMR (101 MHz, $CDCl_3$) δ 172.22, 138.90, 115.33, 68.93, 60.77, 41.23, 14.15 ppm.

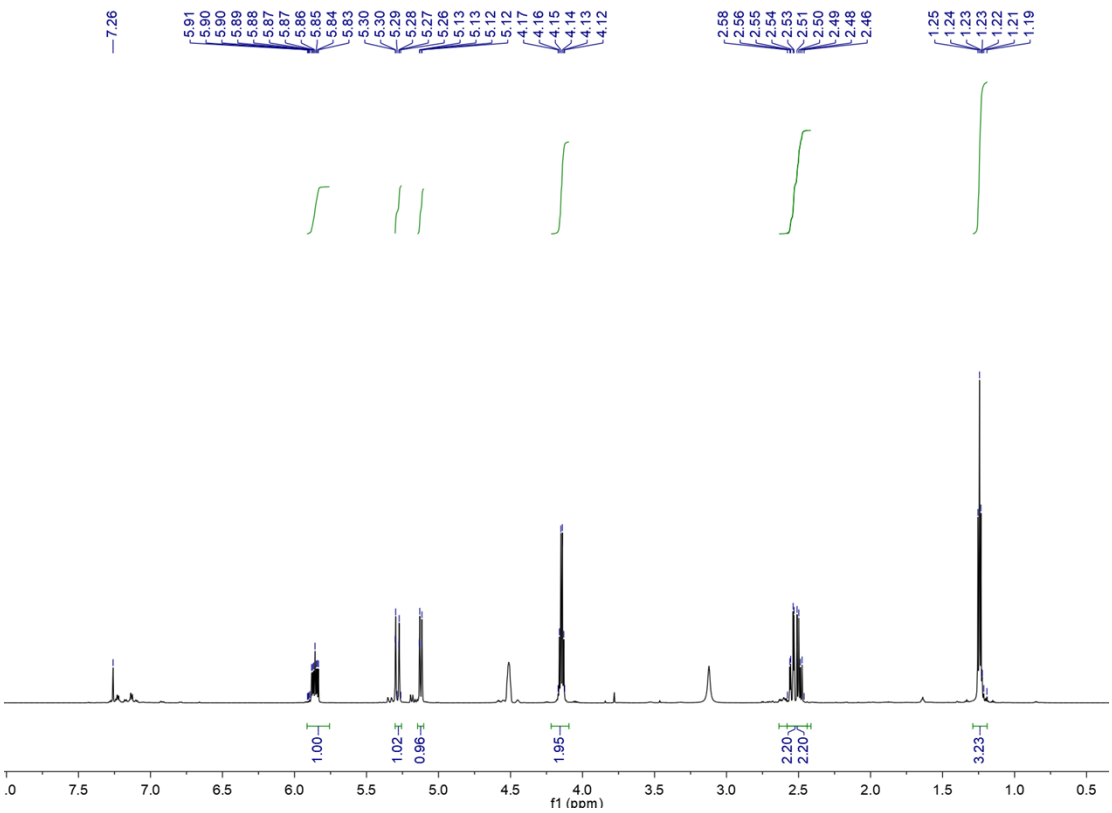

Ethyl 3-hydroxyhexanoate (3e)

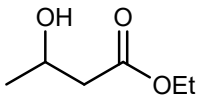

Characterization data:

^{1}H NMR (700 MHz, Chloroform-d) δ 4.16- 4.04 (m, 3H), 2.44 - 2.33 (m, 2H), 1.20 (q, *J* = 7.2, 6.7 Hz, 3H), 1.16 (d, *J* = 6.7 Hz, 3H) ppm.

^{13}C NMR (101 MHz, $CDCl_3$) δ 171.82, 63.26, 59.62, 41.99, 21.53, 13.15 ppm.

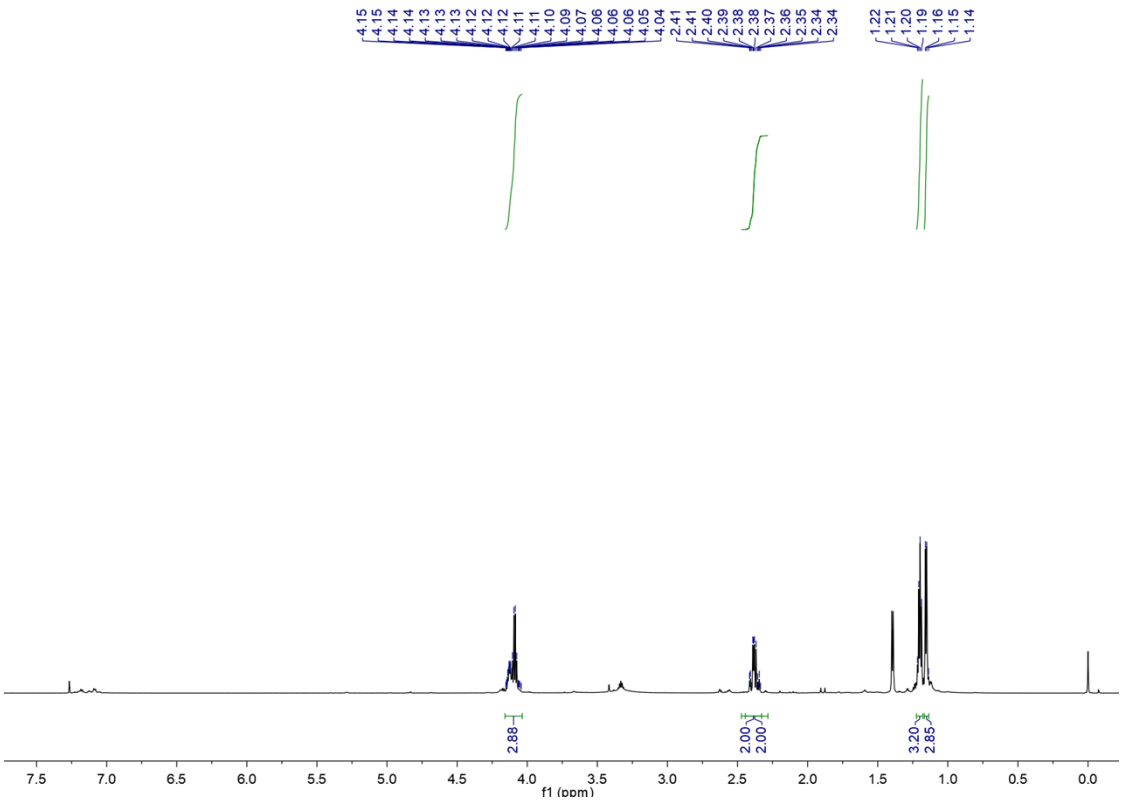

The attached original data of Figures in manuscript

Fig.4a

$t_{add,1}$ (min)	Y_{3a} (%)	η_{2a} (%)
2	57.9	81.3
5	54.9	74.0
10	50.4	65.7

Fig.4b

t_1 (min)	Y_{3a} (%)	η_{2a} (%)
0	57.5	78.8
5	56.8	79.6
10	55.1	71.0
15	50.4	65.7
30	45.8	65.0

Fig.5a

$t_{add,2}$ (min)	Y_{3a} (%)	η_{2a} (%)
2	50.7	70.0
5	51.4	65.7
10	50.4	65.7

Fig.5b

t_1 (min)	Y_{3a} (%)	η_{2a} (%)
1	49.1	63.7
10	51.2	65.6
20	52.1	66.1
30	50.4	64.4
40	48.9	65.8
50	51.0	68.7

Fig.6 Compound 3a

Reaction temperature (^{o}C)	Y_{3a} (%)	η_{2a} (%)
-78	32.6	49.0
20	4.7	6.2

Fig.6 Compound 3b

Reaction temperature (^{o}C)	Y_{3b} (%)	η_{2a} (%)
-78	32.1	42.8

20	4.7	6.0

Fig.10a

Reaction temperature (°C)	Y_{3a} **(%)**	η_{2a} **(%)**
-60	81.4	89.2
-40	87.7	99.8
-20	92.1	98.8
0	72.9	81.4
20	62.3	70.9

Fig.10b

Reaction temperature (°C)	Y_{3a} **(%)**	η_{2a} **(%)**
-20	45.8	84.4
-40	64.4	86.8
-60	90.1	95.3
-78	89.9	99.8

Fig.11a

Q_{EA} **(mL/min)**	Y_{3a} **(%)**	η_{2a} **(%)**
0.5	63.7	65.4
1	74.0	75.7
1.5	82.7	83.9
2.0	92.1	98.8
4.0	92.4	96.0

8.0	93.9	97.5

Fig.11b

Q_{H+} (mL/min)	X_s	t_{mix} (s)
0.5	0.221646001	0.677892407
1	0.129038229	0.382817567
1.5	0.076905056	0.221602158
2.0	0.05170594	0.145697617
4.0	0.019214616	0.051208199
8.0	0.004683424	0.011528027

Fig.12a

t_3 (s)	Y_{3a} (%)	η_{2a} (%)
0.25	85.7	87.2
0.5	85.6	88.6
1	86.9	90.9
5	81.4	89.2
10	84.6	89.3
20	84.0	88.6
40	70.0	74.2

Fig. 12b

t_4 (s)	Y_{3a} (%)	η_{2a} (%)
1	83.3	86.9
30	83.2	86.3
60	81.4	89.2